IJAME

*Int. J. of Applied Mechanics and Engineering, 2024, vol.29, No.4, pp.106-120*
DOI: 10.59441/ijame/194850

# BENDING VIBRATIONS OF A THIN WING FOR A PROFILE WITH TWO AXES OF SYMMETRY

Hoang Thi Minh Thao and Le Thi Thanh*
Department of Mathematics, Faculty of Applied Sciences,
Ho Chi Minh City University of Technology and Education, Ho Chi Minh City, VIETNAM
E-mail: thanhlt@hcmute.edu.vn

In this work, we study the bending vibrations of a thin wing for a profile with two axes of symmetry, taking into account the influence of torsional vibrations on them. The primary focus of the current study is on finding an analytic solution for the wing-bending equation through the Laplace transform, determining the frequency of free-bending vibrations, and constructing the amplitude-frequency response and phase-frequency response of the wing.

**Key words:** torsional vibrations, bending vibrations, airfoil with two axes of symmetry, Mach number, natural frequencies.

## 1. Introduction

Aeroelasticity is a phenomenon that aircraft and rocket engineering have encountered since the twenties of the last century. Their practical significance, complexity and variety of forms in which they occur [2-4] have initiated a large number of studies devoted to various aspects of these phenomena.

From [4-7] and many other works it is known that if there is a dependence of the frequency of free vibrations on the dimensionless speed of the wing relative to the airflow M, divergence and flutter phenomena are possible, that is, loss of stability of the rectilinear shape of the wing, leading to disasters. From a mathematical point of view, there is a loss of stability of the solution to the system of equations of state of the Lyapunov model [8], that is, the development of the wing's own torsional and bending motions according to an unlimited aperiodic law. In [1], the application of Lyapunov stability theory is utilized to identify unstable scenarios of wing torsional vibrations corresponding to the Mach number M. In this paper, by combining Vlasov's theory, bending vibrations will be studied.

Regarding vibrations of aircraft wings, many scientists are interested and recently many studies have been conducted with many different approaches.

In [9] Seher Eken analyzed the free vibration of an aircraft wing based on the thin-walled composite beam theory.

In [10] Pranjal Agrawal, Pankaj Dhatrak, and Paras Choudhary carried out a comparative analysis of aircraft wing vibration characteristics utilizing the finite element method.

Zihao Zhou studied the vibration deformation of an airfoil under harmonic loading caused by fuel weight with finite element methods such as modal analysis and harmonic response analysis used [11].

Evran *et al.* presented a numerical free vibration analysis of airfoils generated using different airfoil cross-sections such as NACA 0009, NACA 2424 and NACA 4415 [12].

In the paper [13] M.S. Maamo *et al.* presented the preliminary results of the study conducted to build a promising system designed to measure the vibration parameters of the aircraft wings. The system's initial simulation results are shown, demonstrating its operability and expected accuracy characteristics, confirming the system's effectiveness and the prospects for the chosen research direction.

* To whom correspondence should be addressed

A.Ya. Zverev and V.V. Chernyh conducted tests to measure the vibration characteristics of a typical fuselage panel from a regional aircraft, as well as the board, flap, and wing structures of an actual aircraft [14]. These tests, which included various vibration-damping configurations, were performed both in reverberation chambers and on a full-scale test bench.

In [15], Guo Yao *et al.* developed the dynamic equation for a plate interacting with yawed subsonic flow using the von Karman nonlinear plate theory and linear potential flow theory, and they analyzed the system's time-varying dynamic properties. The system's natural frequency curve throughout the unfolding process is determined by solving the generalized eigenvalue problem. The time response of the vibration displacement for the thin plate is calculated using the Runge-Kutta method.

## 2. Bending vibrations of a thin wing

### 2.1. Analytical solution of the wing bending equation

Let's consider the equation of bending vibrations:

$$\frac{\partial^4\eta}{\partial\zeta^4}-\frac{\partial^4\eta}{\partial\zeta^2\partial\tau^2}+\frac{1}{r_x^2}\frac{\partial^2\eta}{\partial\tau^2}=K_bC_y^{\alpha}(M)(\alpha+\theta)M^2 . \tag{2.1}$$

Note that this equation is linear inhomogeneous, and the inhomogeneity is generated not only by the presence of a balancing angle of attack $\alpha$ but also by torsional vibrations - the angle of twist $\theta$. To solve this equation, we apply the modal decomposition method [16].

Let us consider the homogeneous equation of bending vibrations:

$$\frac{\partial^4\eta}{\partial\zeta^4}-\frac{\partial^4\eta}{\partial\zeta^2\partial\tau^2}+\frac{1}{r_x^2}\frac{\partial^2\eta}{\partial\tau^2}=0 . \tag{2.2}$$

in which we assume the existence of harmonic vibrations: $\eta(\zeta,\tau)=\eta_a(\zeta)\cdot e^{i\cdot\Omega_I\cdot\tau}$.

The equation for amplitude functions $\eta_a(\zeta)$:

$$\frac{\partial^4\eta_a}{\partial\zeta^4}+\Omega_I{}^2\cdot\frac{\partial^2\eta_a}{\partial\zeta^2}-\frac{\Omega_I{}^2}{r_x^2}\cdot\eta_a(\zeta)=0 . \tag{2.3}$$

We pass from Eq.(2.3) to the system of first-order equations:

$$\begin{cases}\dfrac{\partial}{\partial\zeta}\eta_a(\zeta)=\phi(\zeta),\\[2ex] \dfrac{\partial}{\partial\zeta}\phi(\zeta)=\mu_x(\zeta),\\[2ex] \dfrac{\partial}{\partial\zeta}\mu_x(\zeta)=\Theta(\zeta),\\[2ex] \dfrac{\partial}{\partial\zeta}\Theta(\zeta)=\dfrac{\Omega_I{}^2}{r_x^2}\cdot\eta(\zeta)-\Omega_I{}^2\cdot\mu_x(\zeta).\end{cases} \tag{2.4}$$

Let's move on to matrix notation, introducing the state vector:

$$\psi(\zeta)=\left(\eta_a \quad \phi \quad \mu_x \quad \Theta\right)^T . \tag{2.5}$$

The same system in matrix form has the form:

$$\frac{\partial}{\partial\zeta}\psi(\zeta)=\begin{pmatrix} 0 & 1 & 0 & 0 \\ 0 & 0 & 1 & 0 \\ 0 & 0 & 0 & 1 \\ \dfrac{\Omega_1{}^2}{r^2} & 0 & -\Omega_1{}^2 & 0 \end{pmatrix}\cdot\psi(\zeta). \tag{2.6}$$

The solution in Cauchy form can be easily obtained analytically through the Laplace transform:

$$\psi(\zeta)=V_1(\zeta,\Omega_1)\cdot\psi_0(\Omega_1) \tag{2.7}$$

where $\psi_0(\Omega)$ is the value of the state vector at $\zeta=0$ (vector of initial parameters), the normalized matrix of fundamental solutions $\mathrm{V}_1(\zeta,\Omega)$ is defined as the original matrix defining the Laplace transform of Eq.(2.6) along the $\zeta$ coordinate [16]:

$$V_{1L}(p)=\left[p\cdot\mathrm{I}-\begin{pmatrix} 0 & 1 & 0 & 0 \\ 0 & 0 & 1 & 0 \\ 0 & 0 & 0 & 1 \\ \dfrac{\Omega_1{}^2}{r_x^2} & 0 & -\Omega_1{}^2 & 0 \end{pmatrix}\right]^{-1} \quad ; \quad \mathrm{I}=\begin{bmatrix} 1 & 0 & 0 & 0 \\ 0 & 1 & 0 & 0 \\ 0 & 0 & 1 & 0 \\ 0 & 0 & 0 & 1 \end{bmatrix}. \tag{2.8}$$

Let's denote: $\dfrac{\Omega_1{}^2}{r_x^2}=a$, $\quad \Omega_1{}^2=b$ , here $\dfrac{1}{r_x^2}=\dfrac{A\cdot L^2}{J_x}$ :

$$V_{1L}(p)=\begin{pmatrix} \dfrac{p^3+b\cdot p}{p^4+b\cdot p^2-a} & \dfrac{p^2+b}{p^4+b\cdot p^2-a} & \dfrac{p}{p^4+b\cdot p^2-a} & \dfrac{1}{p^4+b\cdot p^2-a} \\ \dfrac{a}{p^4+b\cdot p^2-a} & \dfrac{p^3+b\cdot p}{p^4+b\cdot p^2-a} & \dfrac{p^2}{p^4+b\cdot p^2-a} & \dfrac{p}{p^4+b\cdot p^2-a} \\ \dfrac{a\cdot p}{p^4+b\cdot p^2-a} & \dfrac{a}{p^4+b\cdot p^2-a} & \dfrac{p^3}{p^4+b\cdot p^2-a} & \dfrac{p^2}{p^4+b\cdot p^2-a} \\ \dfrac{a\cdot p^2}{p^4+b\cdot p^2-a} & \dfrac{a\cdot p}{p^4+b\cdot p^2-a} & \dfrac{-b\cdot p^2+a}{p^4+b\cdot p^2-a} & \dfrac{p^3}{p^4+b\cdot p^2-a} \end{pmatrix}. \tag{2.9}$$

The roots of the denominator:

$$p^4 + b \cdot p^2 - a = 0 \quad \Leftrightarrow \quad p_{1\ldots4} = \begin{pmatrix} \dfrac{\sqrt{\sqrt{b^2 + 4 \cdot a} - b}}{\sqrt{2}} \\ -\dfrac{\sqrt{\sqrt{b^2 + 4 \cdot a} - b}}{\sqrt{2}} \\ i \cdot \dfrac{\sqrt{\sqrt{b^2 + 4 \cdot a} + b}}{\sqrt{2}} \\ -i \cdot \dfrac{\sqrt{\sqrt{b^2 + 4 \cdot a} + b}}{\sqrt{2}} \end{pmatrix}, \tag{2.10}$$

let's denote: $P_1 = \dfrac{\sqrt{\sqrt{b^2 + 4 \cdot a} - b}}{\sqrt{2}}$ ; $P_2 = \dfrac{\sqrt{\sqrt{b^2 + 4 \cdot a} + b}}{\sqrt{2}}$ .

We find the original Eq.(2.9) using the inverse Laplace transform to $p$, obtaining a normalized matrix of fundamental solutions

$$V_1(\zeta, \Omega) = \begin{pmatrix} V_1(\zeta)_{0,0} & V_1(\zeta)_{0,1} & V_1(\zeta)_{0,2} & V_1(\zeta)_{0,3} \\ V_1(\zeta)_{1,0} & V_1(\zeta)_{1,1} & V_1(\zeta)_{1,2} & V_1(\zeta)_{1,3} \\ V_1(\zeta)_{2,0} & V_1(\zeta)_{2,1} & V_1(\zeta)_{2,2} & V_1(\zeta)_{2,3} \\ V_1(\zeta)_{3,0} & V_1(\zeta)_{3,1} & V_1(\zeta)_{3,2} & V_1(\zeta)_{3,3} \end{pmatrix} \tag{2.11}$$

where

$$\begin{aligned}
&V_1(\zeta, \Omega)_{1,1} = \frac{1}{Z} \cdot \left( P_2^2 \cdot \cosh(P_1 \cdot \zeta) + P_1^2 \cdot \cos(P_2 \cdot \zeta) \right), \\
&V_1(\zeta, \Omega)_{1,2} = \frac{1}{Z \cdot \sqrt{a}} \cdot \left( P_2^3 \cdot \sinh(P_1 \cdot \zeta) + P_1^3 \cdot \sin(P_2 \cdot \zeta) \right), \\
&V_1(\zeta, \Omega)_{1,3} = \frac{1}{Z} \cdot \left( \cosh(P_1 \cdot \zeta) - \cos(P_2 \cdot \zeta) \right), \\
&V_1(\zeta, \Omega)_{1,4} = \frac{1}{Z \cdot \sqrt{a}} \cdot \left( P_2 \cdot \sinh(P_1 \cdot \zeta) - P_1 \cdot \sin(P_2 \cdot \zeta) \right), \\
&V_1(\zeta, \Omega)_{2,1} = a \cdot V_1(\zeta, \Omega)_{0,3}, \; V_1(\zeta, \Omega)_{2,2} = V_1(\zeta, \Omega)_{1,1}, \\
&V_1(\zeta, \Omega)_{2,3} = \frac{1}{Z} \cdot \left( P_1 \cdot \sinh(P_1 \cdot \zeta) + P_2 \cdot \sin(P_2 \cdot \zeta) \right),
\end{aligned} \tag{2.12}$$

$$V_1(\zeta,\Omega)_{2,4}=V_1(\zeta,\Omega)_{1,3},\quad V_1(\zeta,\Omega)_{3,1}=a\cdot V_1(\zeta,\Omega)_{1,3},\quad V_1(\zeta,\Omega)_{3,2}=V_1(\zeta,\Omega)_{2,1},$$

$$V_1(\zeta,\Omega)_{3,3}=\frac{1}{Z}\cdot\left(P_1^2\cdot\cosh(P_1\cdot\zeta)+P_2^2\cdot\cos(P_2\cdot\zeta)\right),$$

$$V_1(\zeta,\Omega)_{3,4}=V_1(\zeta,\Omega)_{1,2},\quad V_1(\zeta,\Omega)_{4,1}=a\cdot V_1(\zeta,\Omega)_{3,4},\quad V_1(\zeta,\Omega)_{4,2}=V_1(\zeta,\Omega)_{3,1},\quad \text{cont.(2.12)}$$

$$V_1(\zeta,\Omega)_{4,3}=\frac{1}{Z}\cdot\left(\left(\sqrt{a}\cdot P_2-P_1\cdot b\right)\cdot\sinh(P_1\cdot\zeta)-\left(b\cdot P_2+\sqrt{a}\cdot P_1\right)\cdot\sin(P_2\cdot\zeta)\right),$$

$$V_1(\zeta,\Omega)_{4,4}=V_1(\zeta,\Omega)_{3,3},\quad Z=\sqrt{b^2+4\cdot a}\,.$$

Having analytical expressions for the matrix of fundamental solutions, it is possible to solve a variety of homogeneous and inhomogeneous solutions.

**2.2. Frequencies of free bending vibrations**

Nontrivial solutions of the system exist when the determinant of the matrix expressing the boundary conditions is equal to zero. For a cantilever wing with the origin of coordinates at the centre of gravity of the side profile, the kinematic parameters at the origin of coordinates (dimensionless deflection and angle of rotation) and the end of the cantilever – the force parameters (bending moment and lateral force) are equal to zero. The state vector is determined by two unknown initial parameters $\mu_{x0}$ and $\Theta_0$. Then to determine the frequencies of free vibrations we have the equation:

$$\begin{vmatrix} V_1(1,\Omega)_{3,3} & V_1(1,\Omega)_{3,4} \\ V_1(1,\Omega)_{4,3} & V_1(1,\Omega)_{4,4} \end{vmatrix}=0,$$

$$\begin{aligned}\Rightarrow\frac{\cosh(p_1)^2}{\Omega^2 r_x^4+4}\cdot\Bigg\{&\Omega^2\cdot\left(P_2^2r_x^2+1\right)\cdot\frac{\sin(P_2)^2}{\cosh(P_1)^2}+\Omega^3 r_x^2\cdot\frac{\tanh(P_1)\cdot\sin(P_2)}{\cosh(P_1)}+\\ &+P_2^4\cdot\frac{\cos(P_2)^2}{\cosh(P_1)^2}+P_1^4-\Omega^2\cdot\tanh(P_1)^2\cdot\left(1-P_1^2\cdot r_x^2\right)++2\cdot\Omega^2\cdot\frac{\cos(P_2)}{\cosh(P_1)}\Bigg\}=0,\end{aligned} \tag{2.13}$$

$$P_1=\frac{\sqrt{2\cdot\Omega\cdot\sqrt{\Omega^2\cdot r_x^4+4}-2\cdot\Omega^2\cdot r_x^2}}{2},\quad P_2=\frac{\sqrt{2\cdot\Omega\cdot\sqrt{\Omega^2\cdot r_x^4+4}+2\cdot\Omega^2\cdot r_x^2}}{2}.$$

Equation (2.13) determines the spectrum of free-bending vibrations of the wing.
Calculations were carried out for a wing with aspect ratio $\lambda=10$ and relative thicknesses $\bar{c}=0.05$; $0.1$; $0.15$; $0.2$. Wing material - steel 3: $E=200\ GPa$, $\rho=7850\ kg/m^3$, $\nu=0.3$. Geometric characteristics of two profiles – diamond-shaped (Fig.1a) and "trapezoidal" (Fig.1b), trapezoidal profile parameter $a=0.8$.

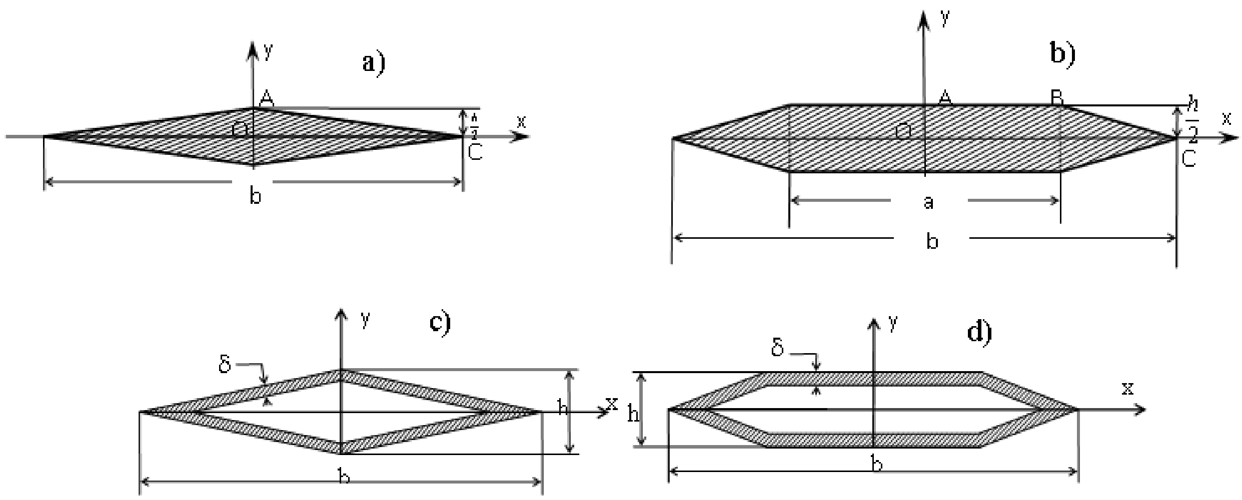


Fig.1. Symmetrical profiles.

Table 1. Dependence of dimensionless radius of inertia on the relative profile thickness.

| Profile | Fig.1a | | | | Fig.1b | | | |
|---|---|---|---|---|---|---|---|---|
| $\overline{c}_t$ | *0.05* | *0.10* | *0.15* | *0.20* | *0.05* | *0.10* | *0.15* | *0.2* |
| $r.10^3$ | *1.201* | *2.041* | *3.062* | *4.082* | *1.403* | *2.805* | *4.208* | *5.611* |

The dependences of the determinant (2.13) on the dimensionless frequency $\Omega$ are shown in Fig.2, and Fig.3. It is clear from them that the first natural bending frequency increases with increasing relative profile thickness and dimensionless radius of inertia during transverse bending. These figures make it possible to determine the isolation intervals of the roots of the frequency Eq.(2.13) for their subsequent refinement. The values of the first natural bending frequency after refinement are shown in Fig.3 and Tab.2.

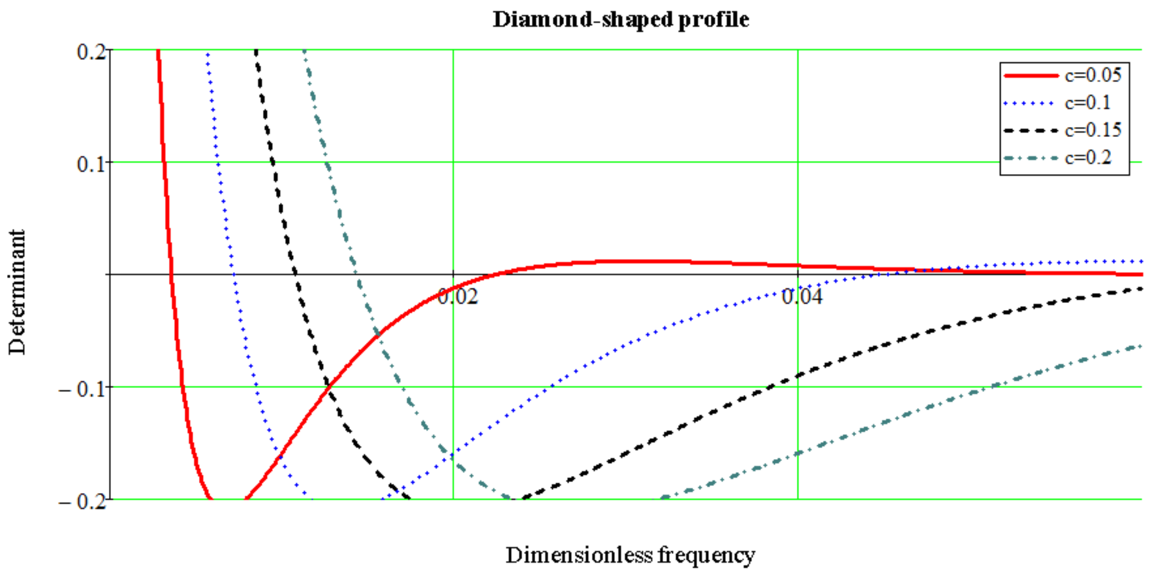


Fig.2. Dependence of the determinant on the dimensionless frequency $\Omega$ for diamond-shaped profile.

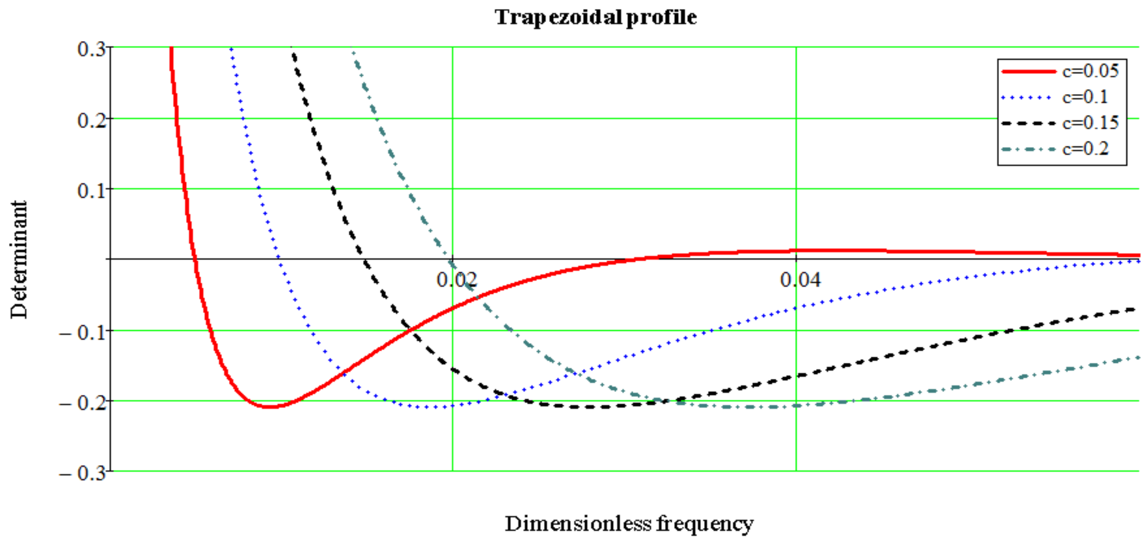


Fig.3. Dependence of the determinant on the dimensionless frequency $\Omega$ for trapezoidal profile.

Table 2. Dependence of the first natural bending frequency on the relative thickness.

| $\bar{c}_t = 0.05$ | | | | |
|---|---|---|---|---|
| Natural frequencies | Fig.1a | Fig.1b | Fig.1c | Fig.1d |
| $\Omega_1$ | 3.516017 | 3.516018 | 3.516017 | 3.516022 |
| $\Omega_2$ | 22.034339 | 22.034203 | 22.034285 | 22.033871 |
| $\Omega_3$ | 61.695739 | 61.694428 | 61.695219 | 61.691216 |
| $\Omega_4$ | 120.895688 | 120.890152 | 120.893491 | 120.87659 |
| $\bar{c}_t = 0.1$ | | | | |
| Natural frequencies | Fig.1a | Fig.1b | Fig.1c | Fig.1d |
| $\Omega_1$ | 3.516022 | 3.516027 | 3.516019 | 3.516045 |
| $\Omega_2$ | 22.033881 | 22.033339 | 22.034157 | 22.03164 |
| $\Omega_3$ | 61.691315 | 61.686072 | 61.693982 | 61.669662 |
| $\Omega_4$ | 120.877008 | 120.854881 | 120.88827 | 120.785662 |
| $\bar{c}_t = 0.15$ | | | | |
| Natural frequencies | Fig.1a | Fig.1b | Fig.1c | Fig.1d |
| $\Omega_1$ | 3.516029 | 3.516042 | 3.51602 | 3.516083 |
| $\Omega_2$ | 22.033119 | 22.031898 | 22.034012 | 22.027878 |
| $\Omega_3$ | 61.683943 | 61.672153 | 61.692583 | 61.633346 |
| $\Omega_4$ | 120.845895 | 120.796163 | 120.88236 | 120.6327 |
| $\bar{c}_t = 0.2$ | | | | |
| Natural frequencies | Fig.1a | Fig.1b | Fig.1c | Fig.1d |
| $\Omega_1$ | 3.51604 | 3.516063 | 3.516022 | 3.516137 |
| $\Omega_2$ | 22.032051 | 22.029882 | 22.033861 | 22.022678 |
| $\Omega_3$ | 61.673626 | 61.652682 | 61.691116 | 61.583236 |
| $\Omega_4$ | 120.802376 | 120.714101 | 120.876168 | 120.422148 |

### 2.3. Forms of free bending vibrations

For each natural frequency, the initial parameters should be found as nontrivial solutions of a homogeneous system of equations

$$\begin{bmatrix} V_1(1,\Omega_k)_{3,3} & V_1(1,\Omega_k)_{3,4} \\ V_1(1,\Omega_k)_{4,3} & V_1(1,\Omega_k)_{4,4} \end{bmatrix} \begin{Bmatrix} \mu_{x0} \\ \Theta_0 \end{Bmatrix} = \begin{Bmatrix} 0 \\ 0 \end{Bmatrix}, \quad k = 1,2,3,4 . \tag{2.14}$$

The rank of this system is $1$, so one of the initial parameters can be set arbitrarily, for example, put $\mu_{x0} = 0$ . Then, eliminating the second equation and determining $\Theta_0$ from the first, we obtain:

$$\Theta_0 = -\frac{V_1(1,\Omega_k)_{3,3}}{V_1(1,\Omega_k)_{3,4}} \mu_{x0} . \tag{2.15}$$

To eliminate arbitrariness in the choice of the parameter $\mu_{x0}$, we take into account that to determine a particular solution to Eq.(2.6), the basis for the expansion of the angle of torsion into a convergent series is the normalized dimensionless transverse displacement $\eta_a(\zeta,\Omega_k)$:

$$\int_0^1 \eta_a(\zeta,\Omega_k)\cdot\eta_a(\zeta,\Omega_m)\,d\zeta = \begin{cases} 1, \forall k = m \\ 0, \forall k \neq m \end{cases}, \quad k,m = 1,\ 2,\ 3... \tag{2.16}$$

This condition serves to determine $\mu_{k0}$:

$$\mu_{k0} = \left\{ \int_0^1 \left[ V_1(\zeta,\Omega_k)_{1,3} - \frac{V_1(1,\Omega_k)_{3,3}}{V_1(1,\Omega_k)_{3,4}} V_1(\zeta,\Omega_k)_{1,4} \right]^2 d\zeta \right\}^{-1/2} . \tag{2.17}$$

Here, to calculate the transverse displacement, expressions for the components of the matrix of fundamental solutions (2.12) and an expression for $\Theta_0$ through $\mu_{x0}$ Eq.(2.15) are used.

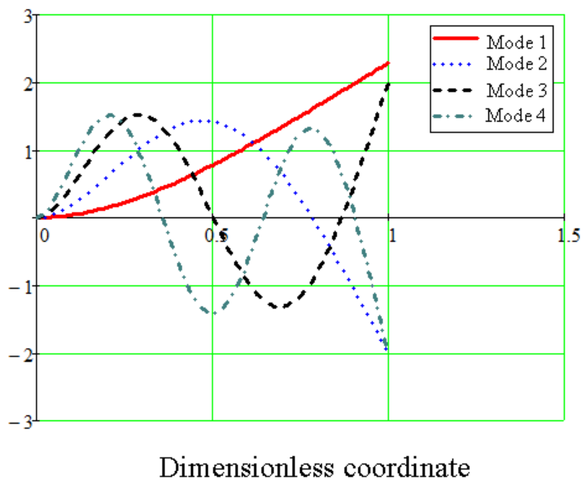


Fig.4. Normalized dimensionless displacement.

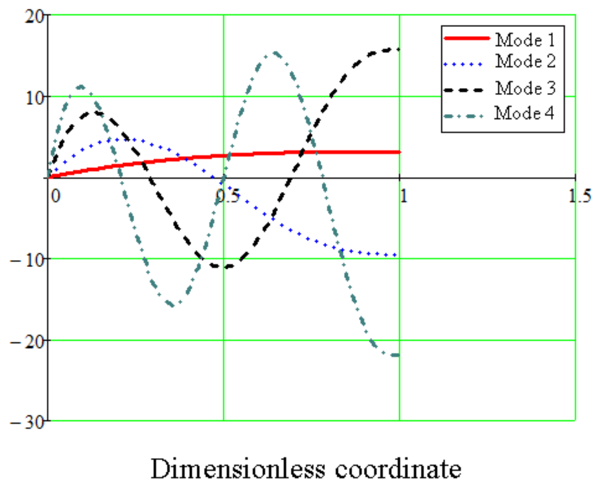


Fig.5. Profile rotation angle.

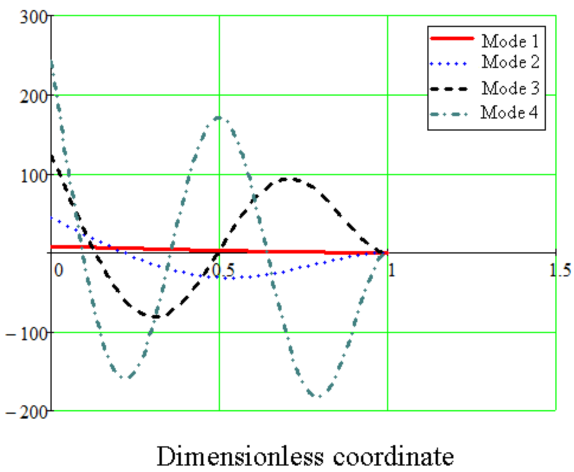


Fig.6. Normalized dimensionless moment.

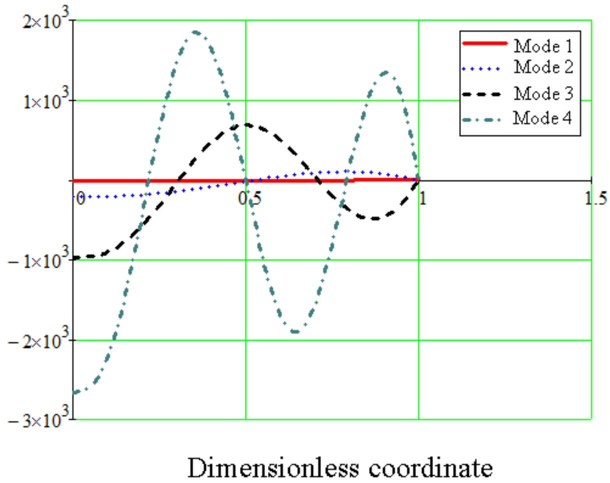


Fig.7. Normalized dimensionless transverse force.

The normalized forms of free bending vibrations shown in Fig.4, by Steklov's theorem, form a complete orthonormal system of functions and can be used as a basis for expanding the right side of the Eq.(2.1).

Figures 5-6 show the components of the wing's bending eigenstates - dimensionless transverse displacement, section rotation angle, dimensionless bending moment and dimensionless transverse force - for the first four natural frequencies. It should be noted that the type of dependence of the eigenstates on the coordinate $\zeta$ is universal for any profile; only the natural frequencies differ.

### 2.4. Solution of the inhomogeneous bending equation

Let us assume that the flow regime is subcritical and the wing performs small torsional oscillations around the balancing value of the angle of attack $\alpha$ with a known first natural frequency $\Omega_1(M)$. We will neglect higher harmonics, since for an elastic wing the first mode of vibration is the most energy-intensive. We will look for a number $M$ at which resonance occurs between bending and torsional vibrations. To be able to estimate the resonant amplitude, we assume that the wing material obeys the Voigt model [17], for which the relationships between stresses and strains have the form:

$$\sigma(t) = E\varepsilon(t) - \mu\dot{\varepsilon}(t), \tag{2.18}$$

or, representing (2.18) in the form of linear-hereditary relations,

$$\sigma(t) = E\varepsilon(t) - \int_0^t \Gamma(t-\tau)\,d\tau, \quad \Gamma(t) = \mu\frac{d\delta(t)}{dt}, \tag{2.19}$$

here Γ(t) is the relaxation kernel, and δ(t) is the Dirac delta function.

Substituting Eq.(2.19) into the bending equation [1] and taking $a_x = 0$, we obtain an equation of the following form:

$$EJ_x\left(\frac{\partial^4 v(t)}{\partial z^4} - \frac{\mu}{E}\int_0^t \Gamma(t-\tau)\frac{\partial^4 v(\tau)}{\partial z^4}d\tau\right) - \rho J_x\frac{\partial^4 v}{\partial z^2 \partial t^2} + \rho A\frac{\partial^2 v}{\partial t^2} = q_y(z,t). \tag{2.20}$$

The external load $q_y(t)$ is represented through the aerodynamic derivative $C_y^{\alpha}(M)$, the angle of attack of the UAV (unmanned aerial vehicle) $\alpha$ and the twist angle $\theta(t)$.

Using the Lagrange-d'Alembert variational equation (since the eigenforms are already known above), we obtain:

$$\int_0^L \left[ \frac{\partial^2 \delta v(z,t)}{\partial z^2} EJ_x \left( \frac{\partial^2 v(z,t)}{\partial z^2} - \frac{\mu}{E} \int_0^t \frac{d}{dt} \delta(t-x) \frac{\partial^2 v(z,x)}{\partial z^2} dx \right) + \right.$$
$$\left. + \delta v(z,t) \rho A \frac{\partial^2 v(z,t)}{\partial t^2} + \frac{\partial \delta v(z,t)}{\partial z} \rho J_x \frac{\partial^3 v(z,t)}{\partial z \partial t^2} - \delta v(z,t) q_y(z,t) \right] dz = 0. \tag{2.21}$$

Moving on to dimensionless variables $z = L\zeta,\ v = L\eta$ and dimensionless time $t = \tau \cdot \frac{L}{r_x} \sqrt{\frac{\rho}{E}}$, we get:

$$\int_0^1 \left[ \frac{\partial^2 \delta\eta(\zeta,\tau)}{\partial \zeta^2} \left( \frac{\partial^2 \eta(\zeta,\tau)}{\partial \zeta^2} - \frac{\mu}{E} \int_0^\tau \frac{d}{d\tau} \delta(\tau-\xi) \frac{\partial^2 \eta(\zeta,\xi)}{\partial \zeta^2} d\xi \right) + \right.$$
$$\left. + \delta\eta(\zeta,\tau) \frac{\partial^2 \eta(\zeta,\tau)}{\partial \tau^2} + \frac{\partial \delta\eta(\zeta,\tau)}{\partial \zeta} r_x^2 \frac{\partial^3 \eta(\zeta,\tau)}{\partial \zeta \partial \tau^2} - \delta\eta(\zeta,\tau) C_y^{\alpha}(M) K_b M^2 \right] d\zeta = 0. \tag{2.22}$$

Let us represent displacement in the form of a modal expansion [16], in which we use eigenfunctions (see above) and their properties as modes:

$$\eta(\zeta,\tau) = \sum_{k=1}^{N} \Psi_{k,1}(\zeta) a_k(\tau), \quad \frac{\partial \eta(\zeta,\tau)}{\partial \zeta} = \sum_{k=1}^{N} \Psi_{k,2}(\zeta) a_k(\tau),$$

$$\frac{\partial^2 \eta(\zeta,\tau)}{\partial \zeta^2} = \sum_{k=1}^{N} \Psi_{k,2}(\zeta) a_k(\tau), \tag{2.23}$$

$$\int_0^1 \Psi_{k,1}(\zeta) \Psi_{m,1}(\zeta) d\zeta = \begin{cases} 1, \forall k = m \\ 0, \forall k \neq m \end{cases}, \quad \int_0^1 \Psi_{k,2}(\zeta) \Psi_{m,2}(\zeta) d\zeta = \begin{cases} \Omega_k^2, \forall k = m \\ 0, \forall k \neq m \end{cases}.$$

Here $\Psi_{k,n}$ are dimensionless state vectors, $k$ is the number of the natural frequency to which the state vector corresponds, $n$ is the number of its components: 1 - displacement, 2 - angle of rotation of the section, 3 - second derivative of displacement (curvature); $a_k$ – modal coefficients – independent functions of time that are not equal to zero at the same time. Note that the variation applies only to $a_k$, since the components of the vector $\Psi$ are considered known. Then from Eq.(2.22), we obtain:

$$\ddot{a}_k - \Omega_k^2 \left[ 1 - \frac{\mu}{E} \int_0^\tau \dot{\delta}(\tau-\xi) a_k(\xi) d\xi \right] = P_k(\tau), \tag{2.24}$$

$$P_k(\tau) = C_y^{\alpha}(M) K_b M^2 \theta_0 \int_0^1 \Psi_{k,1}(\zeta)\theta(\zeta,\tau)d\zeta. \qquad \text{cont.(2.24)}$$

This system of integrodifferential ordinary equations is solved using the integral Laplace transform in time:

$$a_k^*(s) = W_k^*(s)\left[P_k^*(s) + \dot{a}(0) + sa(0)\right],$$

$$W_k^*(s) = \left[s^2(1-C_k) + \Omega_k^2\left(1 - \frac{\mu}{E}s\right)\right]^{-1}, \quad C_k = \int_0^1 \Psi_{k,2}^2(\zeta)d\zeta. \tag{2.25}$$

Here $\dot{a}(0), a(0)$ are the expansion coefficients in a series of eigenfunctions of the initial velocity and initial displacement, which we will consider homogeneous (i.e. equal to zero). The function of the transformation parameter $W_k^*(s)$ in control theory is called the transfer function. If its original is known (the so-called impulse-transition characteristic, ITC), then the originals of the modal coefficients are determined by the Duhamel integral:

$$a_k(\tau) = \int_0^{\tau} W_k(\tau-\xi)P_k(\xi)d\xi. \tag{2.26}$$

For the Voigt model, the original transfer function (ITC) is determined by the expression:

$$W(\tau) = e^{-\beta\tau}\sin(\omega\tau), \quad \omega = \frac{\Omega_k}{2}\sqrt{4 - \left(\frac{\mu}{E}\right)^2 \frac{\Omega_k^2 L^2 \rho}{E}}, \quad \beta = \frac{L}{2r_x}\sqrt{\frac{\rho}{E}}\left(\frac{\mu}{E}\right). \tag{2.27}$$

The parameter $\beta$ has the physical meaning of a logarithmic decrement. For steel 3 it was measured in [18]; its value was *0.2119*.

Let the flight occur at a constant altitude with a constant speed. Due to the linearity of the model, the state of the wing can be represented as a superposition of two states: bending by a constant lift force due to the angle of attack of the UAV (unmanned aerial vehicle), and free torsional vibrations, which can be caused by gusts of wind, changes in density and temperature at flight altitude, etc. Then torsional vibrations can be considered as a monoharmonic external influence with a frequency determined by the first natural frequency of torsional vibrations. Forced bending vibrations at a subcritical number $M$ is the response of the wing to harmonic action, determined by Eq.(2.26) at $\theta(\zeta,\tau) = \theta_1(\zeta)\sin(\Omega_{1tor}\tau)$. Leaving only the steady-state part of the solution, we obtain:

$$A = \frac{1}{\sqrt{\left(\beta^2 + \omega^2 + \Omega_{tor}^2\right)^2 - 4\omega^2\Omega_{tor}^2}}, \quad \phi = arctg\left(\frac{2\beta\Omega_{tor}}{\beta^2 + \omega^2 - \Omega_{tor}^2}\right) \tag{2.28}$$

where $\omega = \Omega_b^f\sqrt{1 - \frac{1}{\left(\Omega_b^f\right)^2}}$ is the natural bending frequency of the elastic wing, $\Omega_b^f$ is the natural bending frequency of the elastic wing, $\Omega_{tor}$ is the frequency of torsional vibrations, $A$ is the amplitude, $\phi$ is the phase of bending vibrations. Formulas (2.28) make it possible to construct the amplitude-frequency response (AFR) and phase-frequency response (PFR) of the wing, in which the role of the external influence frequency is played by the first frequency of free torsional vibrations, varying in the range from 0 (at $M = M_{1tor}$) to $\Omega_{\max}$ ( at $M = 0$ ). The resonant frequency of bending vibrations (corresponding to the maximum AFR), determined from the principle of the derivative of the AFR for the frequency of external influences:

$$\frac{\partial A}{\partial \Omega_{tor}} = \frac{\partial}{\partial \Omega_{tor}} \frac{1}{\sqrt{\left(\beta^2 + \omega^2 + \Omega_{tor}^2\right)^2 - 4\omega^2\Omega_{tor}^2}} = 0, \quad \Omega_{tor}^r = \sqrt{\omega^2 - \beta^2}. \tag{2.29}$$

The corresponding resonant amplitude

$$A_r = \frac{1}{2\beta\sqrt{\Omega_b^2 - 1}} \tag{2.30}$$

where $\Omega_b$ is the dimensionless frequency of free bending vibrations. Note that this amplitude is dimensionless in the sense that it is related to the amplitude of the disturbing lift force:

$$A_\theta = K_b C_y^\alpha(M)\theta_0 M^2 \int_0^1 \Psi_{1,1}(\zeta)\theta_1(\zeta)\,d\zeta \tag{2.31}$$

where $\theta_0$ is the amplitude of torsional vibrations according to their first form, $\theta_1(\zeta)$ is the first normalized natural form of torsional vibrations, $\Psi_{1,1}(\zeta)$ is the first normalized natural form of bending vibrations.

Figure 8 and Fig.9 show the AFR and PFR of the wing at $\beta = 0.2$ , which approximately corresponds to a steel wing. Table 3 shows the values of resonant amplitudes for $\beta = 0.1...0.4$ .

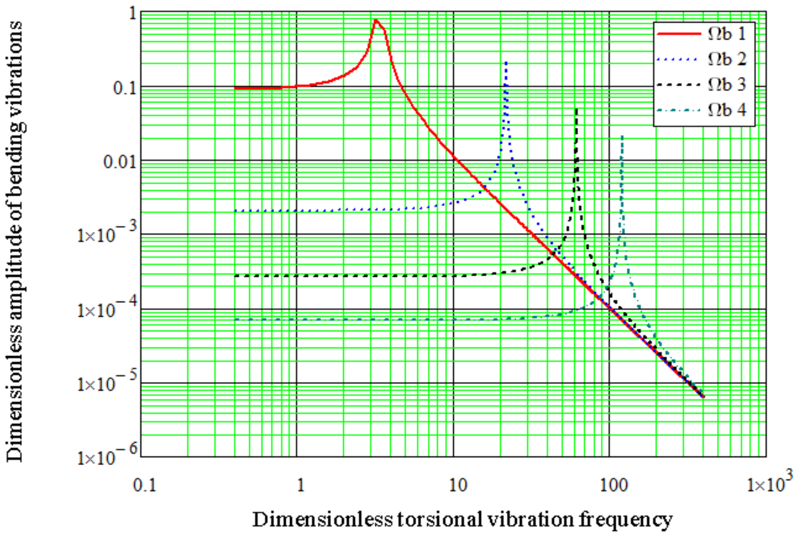


Fig.8. AFR of the wing.

These figures show the AFR and PFR of bending vibrations on four lower modes. The first frequency is dangerous in terms of wing strength since its relative resonant amplitude is the largest of the four for any $\beta$ (see Tab.3).

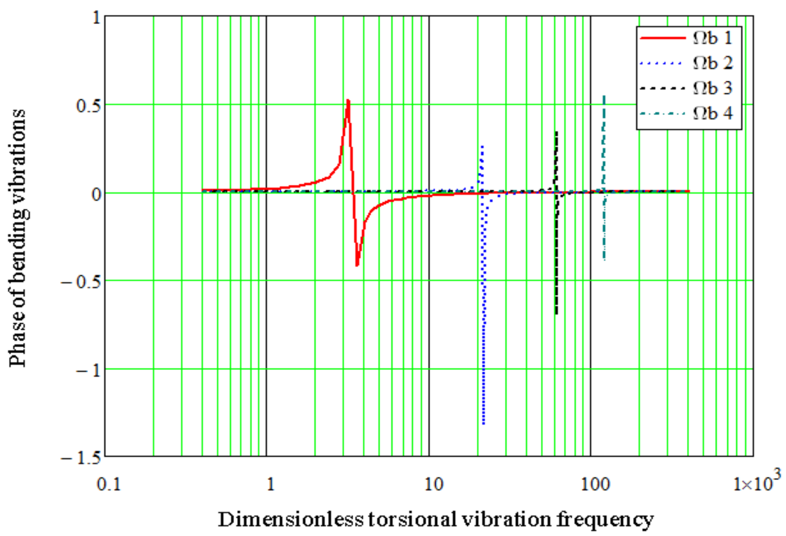


Fig.9. PFR of the wing.

Table 3. Dependence of relative resonant amplitudes on the logarithmic decrement of the material.

| β | N$^{O}$ natural frequency of bending vibrations | | | |
|---|---|---|---|---|
| | *1* | *2* | *3* | *4* |
| *0.1* | *1.483* | *0.227* | *0.081* | *0.042* |
| *0.2* | *0.742* | *0.114* | *0.041* | *0.021* |
| *0.3* | *0.494* | *0.076* | *0.027* | *0.014* |
| *0.4* | *0.371* | *0.057* | *0.02* | *0.01* |

In the PFR (Fig.9), resonance points are characterized by a change in the sign of the phase (from $\pi/2$ to $-\pi/2$), as in any resonant process. The effect of decrement on resonant frequencies is also obvious - an increase in decrement leads to a decrease in the resonant amplitude - and does not contradict the results of other studies of resonant processes [19] with damping proportional to velocity.

Let us consider the results obtained from the point of view of airflow around the wing. As shown in [1], the natural frequencies of torsional vibrations depend on the $M$ number of the free flow, and with increasing $M$ the frequency drops to zero; in Fig.8 is the beginning of the interval. The end of the interval can be chosen quite arbitrarily, but less than the natural frequency of torsional vibrations at $M=0$. Thus, resonance at the first frequency of bending vibrations is possible only near the critical (smallest) number $M$. Resonance at higher frequencies occurs at lower Mach numbers; data [1] and Tab.2 allow us to estimate the first natural frequency of torsional vibrations at $M=0$ with a value of $200...500$, and the fourth frequency of bending vibrations $-120$, then we can assume that the latter corresponds to the descending part of the dependence of the first natural frequency of torsional vibrations on $M$. But its resonant amplitude is the smallest of those given in Tab.3. It is obvious that higher frequencies have even smaller amplitudes and can be neglected.

The process that occurs at $M \approx M_{tor}$ occurs with an aperiodically developing twist angle; the bend, due to the aperiodic right-hand side, will also develop aperiodically, which is easy to establish using the bending ITC Eq.(2.27) and the Duhamel integral Eq.(2.26):

$$a_1(\tau)=\left[\omega\cos(\omega\tau)+\sin(\omega\tau)(\beta+\Omega_{tor})\right]e^{-\beta\tau}-\omega e^{\tau\Omega_{tor}}. \tag{2.32}$$

## 3. Conclusions

The paper has found an analytic solution for the wing-bending equation through the Laplace transform. By finding the solution of the wing-bending equation, natural frequency of free-bending vibrations were determined. The dependence of the natural bending frequency on the relative thickness and material of the wing is also given. The components of the wing's natural states during bending are shown - the dimensionless transverse displacement, the angle of rotation of the section, the dimensionless bending moment and the dimensionless transverse force - for the first four natural frequencies. In addition, the amplitude-frequency response and phase-frequency response of the wing were also established.

### Acknowledgement

This research is supported by Ho Chi Minh City University of Technology and Education (HCMUTE), Vietnam.

## Nomenclature

$A$ – amplitude
$a_k$ – modal coefficients
$A_r$ – resonant amplitude
$\overline{c}$ – relative thickness
$C_y^{\alpha}$ – derivatives of the wing profile's lift coefficient by $\alpha$
$E$ – Young's modulus
$k$ – number of the natural frequency to which the state vector corresponds
$M$ – Mach number
$W(\tau)$ – the original transfer function
$\alpha$ – angle of attack
$\Gamma(t)$ – relaxation kernel
$\eta$ – dimensionless transverse movement
$\eta_a(\zeta)$ – dimensionless deflection (displacement perpendicular to the plane of the wing)
$\theta$ – twist angle
$\Theta(\zeta)$ – dimensionless transverse force
$\lambda$ – aspect ratio
$\mu_x(\zeta)$ – dimensionless bending moment
$v$ – Poisson's ratio
$\zeta$ – dimensionless axial coordinate
$\rho$ – density
$\tau$ – dimensionless time
$\phi$ – the phase of bending vibrations
$\phi(\zeta)$ – angle of rotation of the profile around its main central axis of inertia
$\omega$ – the natural bending frequency of the viscoelastic wing
$\Omega$ – frequencies of free bending vibrations
$\Omega_{tor}$ – the frequency of torsional vibrations

## References

[1] Thanh L.T. (2023): *Determination of the critical velocity of a straight wing with a high aspect ratio*.– International Journal of Applied Mechanics and Engineering, vol.28, No.1, pp.105-117, https://doi.org/10.59441/ijame-2023-0010.

[2] Volmir A.S. (1972): *Nonlinear Dynamics of Plates and Shells*.– Moscow, Science, p.432.

[3] Volmir A.S. (1976): *Shells in Liquid and Gas Flow: Problems of Aeroelasticity*.– Moscow, Science, p.416.

[4] Volmir A.S. (1967): *Stability of Deformable Systems*. – Moscow, Science, p.984.

[5] Fyn Ya. Ts. (1959): *Introduction to The Theory of Aero-stiffness*.– Moscow, State Publishing House of Physical and Mathematical Literature, p. 522.

[6] Vedeneev V.V. (2005): *Flutter of a broad stripe-shaped plate in a supersonic gas flow*.– News of the Russian Academy of Sciences, Mechanics of liquid and gas. No.5. pp. 155-169.

[7] Bolotin V.V. (1961): *Non-conservative Problems of The Theory of Elastic Stability*.– Moscow, State Publishing House of Physical and Mathematical Literature, p.338.

[8] Demidovich B.P. (1967): *Lectures on The Mathematical Theory of Stability*.– Moscow, Nauka, p.532.

[9] Seher Eken (2019): *Free vibration analysis of composite aircraft wings modelled as thin-walled beams with NACA airfoil sections*.– Thin-Walled Structures, vol.139, pp.362-377, https://doi.org/10.1016/j.tws.2019.01.042.

[10] Pranjal Agrawal, Pankaj Dhatrak, Paras Choudhary (2021): *Comparative study on vibration characteristics of aircraft wings using finite element method*.– Materials Today: Proceedings, vol.46, part1, pp.176-183, https://doi.org/10.1016/j.matpr.2020.07.229.

[11] Zhou Z. (2023): *Vibration analysis of airplane wing under fuel weight*.– In: Yadav S., Kumar H., Wan M., Arora P.K., Yusof Y., (eds) Recent Advances in Applied Mechanics and Mechanical Engineering. ICAMME 2022. Lecture Notes in Mechanical Engineering. Springer, Singapore, pp.459-468, https://doi.org/10.1007/978-981-99-2375-5_45.

[12] Evran S., Kurt M., and Kurt A. (2020): *Evaluation of cross-section and wing length in free vibration analysis of aircraft wings*.– Journal of Aviation, vol.4, No.2, pp.17-24, https://doi.org/10.30518/jav.778273.

[13] Maamo M.S., Afonin A.A. and Sulakov A.S. (2022): *Aircraft wing vibration parameters measurement system using MEMS IMUs and closed-loop optimal correction*.– *Aerospace Systems*, vol.5, pp.473-480, https://doi.org/10.1007/s42401-022-00145-x.

[14] Zverev A.Y. and Chernyh V.V. (2022): *Promising methods for reducing the vibrations of aircraft structures under acoustic excitation*.– Dokl. Phys. vol.67, pp.369-376, https://doi.org/10.1134/S1028335822090154.

[15] Guo Yao, Mingjun Song, Lisha Zhu (2023): *Time-varying stability and vibration of an embedded thin plate on a swept wing*.– Aerospace Science and Technology, vol.140, p.108436, https://doi.org/10.1016/j.ast.2023.108436.

[16] Gryazev M.V., Zheltkov V.I., Vasin A.A. and Vasina M.V. (2011): *Applied problems in the mechanics of a deformable solid*.– Statics of Rods. Tula State University Publishing House, part 1, p.112.

[17] Ilyushin A.A. and Pobedrya B.E. (1970): *Fundamentals of The Mathematical Theory of Thermo Viscoelasticity*.– Moscow, Nauka, p.238.

[18] Kholodov A.A. (2009): *Determination of damping characteristics of steel grade steel 3*.– Fundamental and Applied Problems of Engineering and Technology, No.5, pp.12-17.

[19] Iorish Yu.I. (1963): *Vibrometry*.– Moscow, State Scientific and Technical Publishing House of Mechanical Engineering Literature, p.756.

Received: June 13, 2024
Revised: October 18, 2024